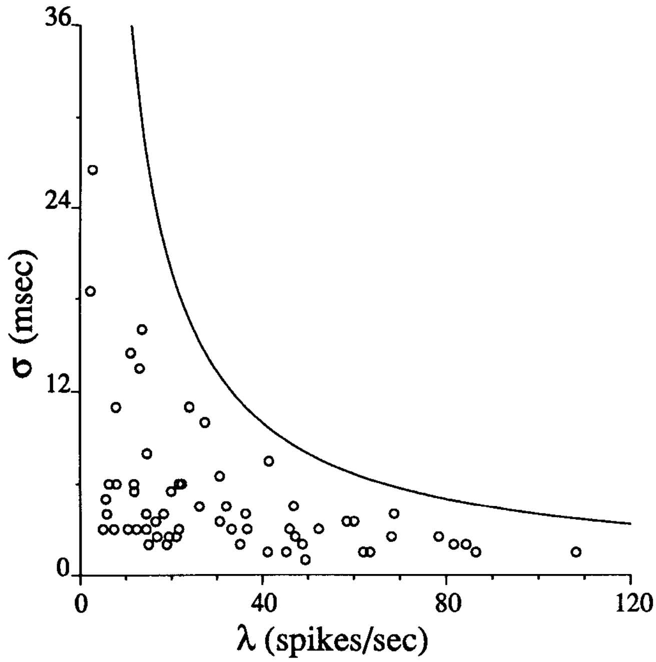

Figure 13. The distribution of parameters for fits of nonburst cells' spectra to the analytical model of the power spectrum of a Poisson process with a refractory period (see Eq. 15). The refractory period parameter σ is plotted against the mean firing rate λ for 61 nonburst cells (*data points*). The *solid line* shows the boundary outside of that the model no longer holds, that is, for which $\lambda > 1/(\sqrt{2\pi}\sigma)$. To the upper right of this line, the firing rate becomes too high to support the corresponding refractory period under our model of the renewal density.

the IBI (interburst interval) distribution; if bursts occur at random but with a fixed absolute refractory period, their distribution should correspond to a shifted exponential, that is, $\mathrm{IBI}(\Delta t) = \gamma e^{-\gamma(\Delta t - t_0)}$ for $t \geq t_0$ and 0 elsewhere, where t_0 is the duration of the absolute refractory period and γ is the mean rate for bursts. If, on the other hand, bursting cells are pacemakers, that is, if they regularly fire in bursts at a fixed interval, the IBI should be sharply peaked around γ. Figure 14 shows the average normalized IBI distribution for 37 cells (those with $p \geq 1.5$ and more than 200 IBIs). The logarithm of the distribution appears linear in the normalized (see Fig. 14 caption) time range of 40–160 msec and falls off at shorter intervals, consistent with a numerical model (thick curves) of Poisson-distributed bursts with a burst-related refractory period that we develop in the next paragraph in terms of a single neuron.

To emulate the data for a single neuron shown in the left column of Figure 15, we synthesize the following point process. Similar to the previous section, we generate "events" using a Poisson process (with $\lambda = 32$ Hz) with a Gaussian-distributed refractory period (of mean 16 msec and 7 msec SD; this distribution was truncated below zero and renormalized). Each event was then replaced with a burst of action potentials, that is, δ-functions, where the length of the burst in milliseconds was approximately Gaussian distributed (mean, 5.2 msec; SD, 1.1 msec) and the spikes within the burst were chosen with approximately Gaussian spacing (mean, 1.8 msec; SD, 0.5 msec). The mean rate λ and the Gaussian refractory distribution were chosen to fit the measured IBI distribution. The parameters of the Gaussian distribution for the length of the burst and the density within the burst were also chosen to fit the neuronal data. If this model is simplified by assuming that the spikes within the bursts are generated by a Poisson process (similar to a model proposed by Smith and Smith, 1965), then the power spectrum would remain flat above 200 Hz, rather than gradually rising as seen at the bottom of Figure 15.

The right column of Figure 15 shows the resultant ISI and power spectrum, which are matched against similar functions for a bursting MT cell (Fig. 15, left column). What is surprising is that the synthetic data shows a peak in the power spectrum at about 31 Hz, *without* any underlying oscillations. How can this occur? A simple analytical model proves to be insightful.

We again appeal to the power function of an infinite train of shot-noise [where each individual shot is described by $h(t)$], with refractory period modeled with the renewal density $p(t)$ (Eq. 13). While before we assumed that individual spikes can best be described using a $\delta(t)$ function, we now model a burst by a boxcar of amplitude A and half-width L centered around the origin. We set L to the half-width of the typical burst and A to normalize the area of the boxcar to account for the number of spikes within the typical burst. The energy spectrum associated with such an event is given by the square of a *sinc* function, that is, by

$$S_h(\omega) = \frac{A^2}{\pi^2}\frac{\sin^2(2\pi Lf)}{f^2} \qquad (16)$$

The power spectrum of such Poisson events with a refractory period is

$$S_{\mathrm{burst}}(f) = \lambda\frac{A^2}{\pi^2}\frac{\sin^2(2\pi Lf)}{f^2}(1 - \sqrt{2\pi}\lambda\sigma e^{-2(\pi f\sigma)^2}), \qquad (17)$$

for $f \neq 0$.

We superimposed $S_{\mathrm{burst}}(f)$ onto the neuron's spectrum in Figure 15 (lower left) and found that both functions show a peak at the same frequency. The reason for the peak is the fact that S_{burst} is the product of $sinc(f)^2$, a decreasing function of f around the origin, and an monotonically increasing function, $1 - e^{-f^2}$. Figure 16 shows the estimated power spectrum $S'(f)$ as well as the associated best fit on the basis of Equation 17 for five burst cells. The analytical model does not account for variations in the burst width and occasional isolated spikes. Also, due to the use of the boxcar function to mimic bursts, we have no control over the fine structure of the spikes within the burst and therefore $S_{\mathrm{burst}}(f)$ does not match well at high frequencies. What is important in this model is that the spectrum of this point process shows a peak, in the absence of any underlying oscillator model. A similar result may be obtained in this case by using IBIs drawn from a broad Gaussian distribution with a mean value close to 25 msec. More neuronal data would be required to distinguish between the appropriateness of these models.

To emphasize the fact that the presence of bursts—in combination with a refractory period—can lead to a peak in the power spectrum, we used all 210 trials at different values of c for one particular cell, *j001*, and replaced every occurrence of a burst by a single spike, located at the center of the burst (Fig. 17). The associated power spectrum changes dramatically in character, from the usual peaked one to a flat spectrum with a dip at low frequency, compatible with the notion that once bursting has been accounted for, what remains are Poisson-distributed events modulated by the presence of a refractory period. If bursts would tend to occur every 25 msec or so, then this procedure should have led to a spectrum with a large peak around 40 Hz. For our data, bursts account satisfactorily for the peaks in the power spectrum. This is also witnessed by the rate of burst occurrence λ, shown in the table in Figure 16, where